

Equivalence of interacting semimetals and low-density many-body systems to single-particle systems with quenched disorder

Shijun Sun¹ and Sergey Syzranov¹

¹*Physics Department, University of California, Santa Cruz, California 95064, USA*

Describing collective behaviour of a large number of interacting particles is one of the biggest challenges in physics and is key to understanding phase transitions and transport and thermodynamic properties in systems with strong particle correlations. We demonstrate that a broad class of interacting disorder-free systems, such as nodal semimetals (e.g. graphene, Weyl, nodal-line semimetals) and dilute interacting gases, can be mapped to non-interacting systems with quenched disorder. The interacting systems that allow for such a mapping include systems with a small single-particle density of states at the chemical potential (e.g. near the nodal point or a nodal line in a topological semimetal), which leads to a suppressed screening of the interactions. The established duality suggests a new approach for analytical and numerical studies of many-body phenomena in a class of interacting disorder-free systems by reducing them to single-particle problems. It allows one to predict, describe and classify many-body phenomena by mapping them to the effects known for disordered non-interacting systems. We illustrate the mapping by showing that clean semimetals with attractive interactions exhibit interaction-driven transitions at low temperatures in the same universality classes as the non-Anderson disorder-driven transitions predicted in high-dimensional non-interacting semimetals. Furthermore, we find a new non-Anderson disorder-driven transition dual to a previously known interaction-driven transition in clean bosonic gases. The established principle may also be used to classify and describe phase transitions in dissipative systems described by non-Hermitian Hamiltonians.

Describing many-body interacting systems is one of the greatest challenges in physics. Often, existing analytical approaches are insufficient to accurately describe many-body effects, such as high-temperature superconductivity, interaction-driven metal-insulator transition and magnetic phase transitions.

Simulating such systems numerically also is a formidable task, in the case of fermionic (quasi-)particles, due to the notorious sign problem^{1–3}, which leads to a rapid growth of the required computing time with the number of particles. By contrast, single-particle problems, even in the presence of quenched disorder, may be comparatively easily simulated, e.g., by diagonalising the Hamiltonian of the system.

Disorder-averaged observables in single-particle models, however, are described by interacting field theories, in the supersymmetric⁴, Keldysh⁵ or replica⁶ representations. Such theories have the same form as the field theories for interacting disorder-free systems, but have additional structures in, respectively, boson-fermion, Keldysh or replica subspaces. It is natural to expect, therefore, that a certain class of many-body systems may be mapped to single-particle disordered models.

Such a mapping would allow one to easily simulate numerically many-body phenomena in these systems, by mapping them to models with quenched disorder and without interactions. Furthermore, it would allow to predict new many-body phenomena, e.g. phase transitions, dual to the previously known disorder-driven phenomena in the corresponding single-particle models. The purpose of this paper is to investigate such a duality between interacting and disordered non-interacting systems and explore the respective classes of systems.

Naively, the Matsubara field theory for a d -dimensional

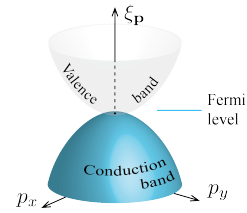


FIG. 1. The band structure of a nodal semimetal.

interacting system with the four-particle interaction decoupled by a Hubbard-Stratonovich field^{2,7} $u(\tau, \mathbf{r})$ appears to have the same structure as the field theory of a single-particle system with a random potential u , if the Matsubara time τ is considered as one of the coordinates. However, the effective Hamiltonian of the latter theory is non-Hermitian and, thus, does not correspond to realistic systems with quenched disorder. Furthermore, the corresponding partition function rapidly oscillates as a function of the random potential for fermionic particles, which constitutes the numerical sign problem^{1–3}.

In this paper, we demonstrate that a class of d -dimensional disorder-free systems with attractive interactions, such as nodal semimetals (Weyl/Dirac, semi-Dirac and nodal-line semimetals) and dilute gases, may be mapped to $d + 1$ -dimensional disordered non-interacting systems with an additional (pseudospin) degree of freedom equivalent to a spin-1/2. The interacting systems that allow for such a mapping include systems with a low density of states at the chemical potential, e.g., near a band edge or a band touching point in a nodal or nodal-line semimetals (see Fig. 1), which allows to neglect the effect of the screening of the interactions on transport and thermodynamic observables.

The existence of this mapping is consistent with the well-known² absence of the numerical problem in systems with particle-hole symmetry. Indeed, the conduction and the valence bands in nodal semimetals touch in momentum space, which is why they have particle-hole or approximate particle-hole symmetry if the bands are symmetric and the chemical potential lies close to the nodal line or point.

Another distinctive feature of nodal semimetals and dilute gases with the dispersion $\xi_{\mathbf{k}} \propto k^\alpha$ near a node or a band edge is the vanishing of the single-particle density of states (DoS) $\propto E^{\frac{d}{\alpha}-1}$ in dimensions $d > \alpha$. Low density of states leads to the suppression of the screening of the interactions between the particles. Although the interactions may still be screened even for zero DoS at the chemical potential, the screening may often be neglected, for example, when computing transport coefficients in intrinsic graphene^{8,9,10} or Weyl semimetals. The screening of effective interactions is also absent in the deterministic field theories^{5-7,11} of disordered systems, which suggests the existence of the mapping to interacting systems at all orders of the perturbation theory.

This mapping suggests, in particular, that interacting electronic systems with a vanishing DoS at the Fermi level exhibit interaction-driven phase transitions in the universality classes of the non-Anderson disorder-driven phase transitions¹²⁻¹⁸ that have been established, at the perturbative level, to take place in non-interacting semimetals in high spacial dimensions, exemplified by 3D Weyl semimetals. Using the duality demonstrated in this paper, we find also a new non-Anderson disorder-driven phase transition.

Summary of the mapping. We consider d -dimensional interacting systems described by Hamiltonians of the form

$$\hat{\mathcal{H}} = \int \hat{\Psi}^\dagger(\mathbf{r}) \xi_{\hat{\mathbf{p}}} \hat{\Psi}(\mathbf{r}) d^d \mathbf{r} - \frac{1}{2} \int \hat{\Psi}^\dagger(\mathbf{r}) \hat{\Psi}^\dagger(\mathbf{r}') U(\mathbf{r} - \mathbf{r}') \hat{\Psi}(\mathbf{r}') \hat{\Psi}(\mathbf{r}) d^d \mathbf{r} d^d \mathbf{r}', \quad (1)$$

where $\hat{\Psi}^{(\dagger)}$ are the particle annihilation (creation) operators; $\xi_{\hat{\mathbf{p}}}$ is the dispersion of the particles; $\hat{\mathbf{p}} = -i\partial_{\mathbf{r}}$ is the momentum operator (hereinafter $\hbar = 1$) and the potential $U(\mathbf{r} - \mathbf{r}')$ describes the interactions in the system.

In this paper, we focus on systems with the power-law dispersion $\xi_{\hat{\mathbf{p}}} \propto p^\alpha$ with $\alpha < d$ near a band edge or a node (band touching point) which may also have additional structure in the spin or valley space. $\alpha = 1$ corresponds to graphene for $d = 2$ and to 3D Weyl/Dirac semimetals for $d = 3$. The case $\alpha = 2$ is realised in semiconductors and parabolic semimetals. Dispersions with a continuously tunable parameter α may be realised in systems of trapped ultracold particles¹⁹⁻²² and superconductive films²³. Furthermore, it has been demonstrated²⁴ that d -dimensional systems with long-range hopping $\propto 1/r^{d+\alpha}$, also realised with trapped ultracold particles, are dual to systems with the power-law dispersion $\xi_{\hat{\mathbf{p}}} \propto p^\alpha$. In what follows, we assume that the screening of the interactions

may be neglected for the quantities of interest due to the vanishing of the DoS at low energies for $d > \alpha$.

In the case of short-range interactions, on which we focus in this paper (for a generalisation to the case of more generic interactions see Appendix A), the strength of the interactions may be characterised by one coupling constant

$$g = \int U(\mathbf{r} - \mathbf{r}') d^d \mathbf{r}'. \quad (2)$$

The Hamiltonian (1) may describe both bosonic and fermionic particles. While we consider, for simplicity, spinless particles, the mapping described in this paper may be generalised to account for an arbitrary spin structure of the dispersion and the interaction.

We demonstrate that the behaviour of observables in an interacting disorder-free d -dimensional system described by the Hamiltonian (1) with short-range unscreened interactions can be mapped to the behaviour of disorder-averaged observables in a $d + 1$ non-interacting semimetal with the Hamiltonian

$$\hat{h} = \hat{\sigma}_z \xi_{\hat{\mathbf{p}}} + \hat{\sigma}_y p_{d+1} + \hat{\sigma}_z u(\boldsymbol{\rho}), \quad (3)$$

where $\hat{\sigma}_x$, $\hat{\sigma}_y$ and $\hat{\sigma}_z$ are the Pauli matrices corresponding to a degree of freedom equivalent to a spin-1/2, hereinafter referred to as *pseudospin*; \mathbf{p} is the momentum of the particle along the first d dimensions; p_{d+1} is the component of momentum along the $d + 1$ -st dimension and $u(\boldsymbol{\rho})$ is short-range-correlated random potential characterised by the same coupling constant (disorder strength)

$$g = \int \langle u(\boldsymbol{\rho}) u(\boldsymbol{\rho}') \rangle_{\text{dis}} d^{d+1} \boldsymbol{\rho}', \quad (4)$$

where $\boldsymbol{\rho}$ and $\boldsymbol{\rho}'$ are locations in the $d + 1$ -dimensional space.

For example, the average density $\hat{n}(\mathbf{r}) = \hat{\Psi}^\dagger(\mathbf{r}) \hat{\Psi}(\mathbf{r})$ of particles in the interacting system matches, as a function of the coupling g , the disorder-averaged observable

$$\rho_s(\boldsymbol{\rho}) = \frac{1}{4} \text{Tr} \left[\hat{\sigma}_z \hat{G}^R(\boldsymbol{\rho}, \boldsymbol{\rho}, 0) + \hat{\sigma}_z \hat{G}^A(\boldsymbol{\rho}, \boldsymbol{\rho}, 0) \right] \quad (5)$$

in the dual disordered non-interacting system, where Tr is taken over the pseudospin degree of freedom and $\hat{G}^R(\boldsymbol{\rho}, \boldsymbol{\rho}, E)$ and $\hat{G}^A(\boldsymbol{\rho}, \boldsymbol{\rho}, E)$ are the matrices of the retarded and advanced Green's functions of the particles in the pseudospin space. The correspondence between various quantities in the interacting disorder-free and non-interacting disordered models described, respectively, by the Hamiltonians (1) and (3), is summarised in Table I.

In this paper, we focus on the case of a positive coupling g , which corresponds to the real random potential $u(\boldsymbol{\rho})$ and, accordingly, attractive interactions in the Hamiltonian (1). In the case of repulsive interactions, $g < 0$, the mapping leads to an imaginary potential in the Hamiltonian (3) of the disordered system. The corresponding non-Hermitian Hamiltonians are sometimes

	Interacting model	Disordered model
Coordinates	(τ, \mathbf{r})	(τ_{d+1}, \mathbf{r})
Temperature/size	T	$1/\ell_{d+1}$
Coupling to interactions/disorder	$\hat{\Psi}^\dagger \hat{\Psi} \phi$	$\hat{\psi}^\dagger \hat{\sigma}_z \hat{\psi} u$
Observables	\hat{n} (density)	ρ_s , Eq. (5)

TABLE I. Correspondence between quantities in the interacting disorder-free and non-interacting disordered systems

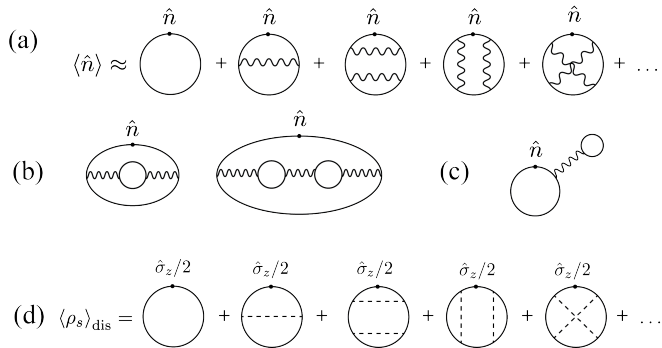


FIG. 2. Diagrams for observables in dual interacting disorder-free and non-interacting disordered systems. (a) Contributions to the concentration of particles in the interacting system. (b)-(c) Examples of neglected contributions; diagrams (b) are neglected due to the suppressed screening; (c) is the Hartree contribution. (d) Corresponding contributions to the disorder-averaged quantity ρ_s , given by Eq. (5) in the disordered non-interacting system.

used to describe dissipative systems or systems which allow for loss or gain of particles^{25–29}.

Derivation of the duality. We consider, perturbatively in the interaction, the average concentration \hat{n} of the particles in the interacting systems and show its mapping to the respective observable (5) in the non-interacting disordered system. The mapping may be demonstrated similarly for any correlator of the concentrations \hat{n} or other observables, e.g. currents.

All perturbative contribution to the equilibrium value

$$\begin{aligned}
& \frac{g^N}{V^{N+1} \ell_{d+1}^{N+1}} \sum_{\mathbf{p}, k} \text{Tr} \left[\hat{\sigma}_z \frac{1}{-k_0 \hat{\sigma}_y - \xi_{\mathbf{p}_0} \hat{\sigma}_z} \frac{1}{2} \frac{\hat{\sigma}_z}{-k_0 \hat{\sigma}_y - \xi_{\mathbf{p}_0} \hat{\sigma}_z} \frac{1}{\hat{\sigma}_z} \frac{1}{-k_1 \hat{\sigma}_y - \xi_{\mathbf{p}_1} \hat{\sigma}_z} \hat{\sigma}_z \dots \hat{\sigma}_z \frac{1}{-k_{2N-1} \hat{\sigma}_y - \xi_{\mathbf{p}_{2N-1}} \hat{\sigma}_z} \right] \\
& = \frac{g^N}{2V^{N+1} \ell_{d+1}^{N+1}} \sum_{\sigma_x = \pm 1} \sum_{\mathbf{p}, k} \frac{1}{(i\sigma_x k_0 - \xi_{\mathbf{p}_0})^2} \frac{1}{i\sigma_x k_1 - \xi_{\mathbf{p}_1}} \dots \frac{1}{i\sigma_x k_{2N-1} - \xi_{\mathbf{p}_{2N-1}}}, \quad (7)
\end{aligned}$$

where we have introduced the length $\ell_{d+1} = 1/T$ of the disordered system along the $d+1$ -st dimension ($V \ell_{d+1}$ is the volume of this $d+1$ -dimensional system); k_i is the momentum along this dimension. In Eq. (7), we took

of $\langle \hat{n} \rangle$ correspond to the diagrams in Fig. 2a. They include, apart from the interaction propagators shown by wiggly lines, only one loop of particle propagators. Under the made approximations, we neglect the contributions with additional loops of particle propagators, exemplified by diagrams 2b-c. Some of those contributions (shown in Fig. 2b) correspond to the screening of the interactions. The other contributions contain a loop connected to the rest of the diagram by a single interaction propagator (Hartree-type contributions, shown in Fig. 2c). Such contributions are responsible for the renormalisation of the chemical potential and do not affect other observables. In what follows, we consider the quasiparticle dispersion to be measured from a given chemical potential and thus disregard such Hartree contributions.

The contribution of each diagram with N interaction propagators is given by

$$\frac{T^{N+1} g^N}{V^{N+1}} \sum_{\omega, \mathbf{p}} \frac{1}{(i\omega_0 - \xi_{\mathbf{p}_0})^2} \frac{1}{i\omega_1 - \xi_{\mathbf{p}_1}} \dots \frac{1}{i\omega_{2N-1} - \xi_{\mathbf{p}_{2N-1}}}, \quad (6)$$

where V is the volume of the interacting (d -dimensional) system; ω_i and \mathbf{p}_i with $i = 0, 1, \dots, 2N-1$, are the frequency and momenta of the particle propagators subject to N linear constraints due to energy and momentum conservation; $\sum_{\omega, \mathbf{p}} \dots$ is summation over all independent frequencies and momenta. For bosonic (fermionic) particles, $\omega_i = 2\pi T n_i$ [$\omega_i = \pi T(2n_i + 1)$], where n_i is an integer (hereinafter $k_B = 1$). Here, we assume for simplicity that the interactions are short-ranged and replace all interaction propagators by frequency- and momentum-independent constants g . Our results hold, however, for a generic spatial and time dependence of the interactions (see Appendix A).

Each diagram for the interacting system in Fig. 2a corresponds to a topologically equivalent diagram in Fig. 2d for the disorder-averaged observable $\langle \rho_s \rangle_{\text{dis}}$ in the $d+1$ -dimensional disordered non-interacting system described by the Hamiltonian (3). Each diagram of order N for the average value of the operator (5) is given by (see Appendix A for more details)

into account that the observable ρ_s given by Eq. (5) corresponds to the vertex $\hat{\sigma}_z$ and the zero-energy particle propagator $\frac{1}{2}[G^R + G^A](k_i, \mathbf{p}_i) = (-k_i \hat{\sigma}_y - \xi_{\mathbf{p}_i} \hat{\sigma}_z)^{-1}$ (see Appendix A for details of the diagrammatic technique).

The boundary conditions along the $d+1$ -st dimension are chosen to be (anti)periodic if the dual interacting system is (fermionic) bosonic, leading to quantised momenta k_i that match the Matsubara frequencies ω_i in Eq. (6). Because the expression (7) for the diagram in the disordered system is invariant with respect to inverting the signs of all momenta k_i , it matches Eq. (6) that gives the value of the topologically equivalent diagram in the interacting system. This demonstrates that the density of particles $\langle \hat{n} \rangle$ in the interacting systems matches the quantity $\langle \rho_s \rangle_{\text{dis}}$ in the disordered system at all orders of the perturbation theory in the coupling g . Similarly, one may demonstrate the mapping between correlators of the respective operators and between other observables in the interacting disorder-free and non-interacting disordered systems described by the Hamiltonians (1) and (3).

Interactions-disorder duality in nodal semimetals and phase transitions. The described mapping suggests a duality between interacting d -dimensional semimetals with the dispersion $\xi_{\mathbf{k}} \propto k^\alpha$ near the node, where $\alpha < d$, and disordered non-interacting $d+1$ -dimensional semimetals with the dispersion $\xi_{\mathbf{k}} \hat{\sigma}_z + k_{d+1} \hat{\sigma}_y$. This allows to classify and describe, e.g., phase transitions in interacting semimetals using the results established for the dual disorder-driven transitions in non-interacting systems and vice versa.

Nodal semimetals may display a variety of instabilities and associated phase transitions at low temperatures (see, for example, Refs. 30–36), including, but not limited to, superconductive, magnetic and charge-density-wave phase transitions. By contrast, non-interacting disordered systems are commonly believed to exhibit only one phase transition: the Anderson localisation-delocalisation transition. However, it has been demonstrated, at the perturbative level, that semimetals and semiconductors with the power-law dispersion $\propto k^\delta$ in high dimensions $\tilde{d} > 2\delta$ exhibit additional disorder-driven transitions (see Ref. 14 for a review) in non-Anderson universality classes. These non-Anderson disorder-driven transitions may have diverse properties depending on the symmetries of disorder and of the band structure. The phenomenology of the non-Anderson disorder-driven transitions may be generalised to anisotropic dispersions, including those of the Hamiltonians of the form $\xi_{\mathbf{k}} \hat{\sigma}_z + k_{d+1} \hat{\sigma}_y$ [cf. Eq. (3)] with $\xi_{\mathbf{k}} \propto k^\alpha$. Such Hamiltonians describe, for example, 2D and 3D semi-Dirac semimetals (dual to 1D and 2D interacting systems with the quadratic dispersion, $\xi_{\mathbf{k}} \propto k^2$) and graphene (dual to a Luttinger liquid, $\xi_{\mathbf{k}} = k \hat{\tau}_z$). The corresponding lower critical dimension is $\tilde{d}_c \equiv d_c + 1 = \alpha + 1$.

At such transitions, the single-particle DoS plays the role of the order parameter^{17,18,37–50}: it is finite on one side of the transition and vanishes on the other side, so long as exponentially rare non-perturbative contributions^{51–53,18,44,54,55} (rare-region effects) are neglected. Rare-region effects may broaden this non-Anderson criticality, thus converting the transition to a sharp crossover,

as has been demonstrated numerically in 3D Dirac/Weyl semimetals^{44,54}. The corresponding transitions in the dual interacting systems, however, may be true phase transitions because the described mapping has been established at the perturbative level and does not take into account non-perturbative (instantonic) contributions to observables.

The critical behaviour near phase transitions in both disorder-free interacting and disordered non-interacting systems, described respectively by the Hamiltonians (1) and (3), may be understood from the renormalisation-group (RG) analysis of the dimensionless coupling constant

$$\gamma = \frac{\zeta S_d}{2(2\pi)^d} g K^{d-\alpha}, \quad (8)$$

where S_d is the volume of a unit d -dimensional sphere; K is the ultraviolet momentum cutoff, e.g. the characteristic size of the band in momentum space; ζ is a factor of order unity that depends on the spin and valley structure of the dispersion near the node or the band edge ($\zeta = 1$ for $\xi_{\mathbf{k}} = k^\alpha$). Upon integrating out the highest momentum modes of the particles in both systems (see Appendix B), the RG flow of the dimensionless coupling for the remaining lower-momentum modes is given by the equation

$$\partial_t \gamma = (\alpha - d)\gamma + \gamma^2, \quad (9)$$

which signals a phase transition (in systems with attractive interactions, $g > 0$) which occurs in high dimensions $d > \alpha$ at the critical coupling $\gamma_c = d - \alpha$ and has the correlation-length exponent $\nu = (d - \alpha)^{-1}$.

This renormalisation and the concomitant interaction-driven transition have been first derived⁵⁶ in the context of dilute Bose gases with attractive interactions near the Feshbach resonance^{57–59}. The mapping developed in this paper demonstrates that dual disorder-driven transitions take place in systems non-interacting disordered semimetals with the dispersions $\propto k^\alpha \hat{\sigma}_z + k_{d+1} \hat{\sigma}_y$ in dimensions $\tilde{d} > \alpha + 1$ (see Appendix B for the straightforward RG analysis for such semimetals). We note that such non-Anderson disorder-driven transitions are distinct from the previously studied¹⁴ non-Anderson disorder-driven transitions (they, e.g., lie in a different universality class) and, to our knowledge, are obtained here for the first time based on the duality mapping derived in this paper.

Recently, it has been demonstrated numerically⁶⁰ for a 1D model, which exhibits a high-dimensional non-Anderson disorder-driven transition with the criticality controlled by a small parameter ε , that its correlation-length exponent $\nu = \frac{3}{2|\varepsilon|} + \mathcal{O}(1)$ is different from the prediction $\nu_{RG} = 1/|\varepsilon|$ of the perturbative one-loop RG analysis which is expected to be exact in the limit $\varepsilon \rightarrow 0$. This discrepancy may signal spontaneous generation of relevant operators that have been overlooked in all previous studies of the non-Anderson disorder-driven transitions. The mapping between interacting disorder-free

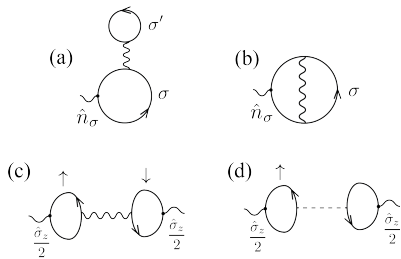


FIG. 3. Diagrams for correlations in the one-site Hubbard model and a disordered wire. Diagrams (a) and (b) describe modifications to the number n_σ of the particles with spin σ , but do not affect the correlations between n_\uparrow and n_\downarrow mimicked by diagram (c) to the first order in the interaction g . Diagram (d) describes correlations in the dual non-interacting disordered system.

and non-interacting disordered systems derived in this paper prompts, therefore, a revision of the results for instabilities in interacting nodal semimetals, as well as investigating the role of non-perturbative contributions to observables.

Duality between a quantum dot and a 1D disordered wire. Even if the assumptions about the negligibility of the screening of the interactions is not fulfilled, the mapping described in this paper still manifests itself in the duality between observables in disordered and interacting systems if those observables are unaffected (to a given accuracy) by the screening and Hartree-type contributions. To illustrate this, we consider a one-site Hubbard model (quantum dot) described by the Hamiltonian

$$\hat{\mathcal{H}}_{dot} = \xi \hat{n}_\uparrow + \xi \hat{n}_\downarrow - g \hat{n}_\uparrow \hat{n}_\downarrow, \quad (10)$$

where ξ is a constant and n_\uparrow and n_\downarrow are the numbers of the electrons in the “spin up” and “spin down” states. With regard to the mapping derived in this paper, this quantum dot is dual to a system of 1D particles in a random potential $u(x)$, with the Hamiltonian given by

$$\hat{h}_{wire} = \sum_{i=\uparrow,\downarrow} \hat{\Psi}_i(x) [\xi \hat{\sigma}_z - i \hat{\sigma}_y \partial_x + u(x) \hat{\sigma}_z] \hat{\Psi}_i(x). \quad (11)$$

Strictly speaking, the interacting systems with the Hamiltonian (10) does not satisfy the assumptions we used to derive the mapping: in general, the contributions that mimic the screening of the interactions and

the Hartree contributions are not negligible. For example, the Hartree contribution in Fig. 3a matches the value of diagram 3b. These contributions, however, do not affect, to the first order in the coupling g , the correlator

$$K = \langle \hat{n}_\uparrow \hat{n}_\downarrow \rangle - \langle \hat{n}_\uparrow \rangle \langle \hat{n}_\downarrow \rangle \quad (12)$$

of the numbers of fermions with different spins. The value of the correlator (12) matches, to the leading order in g , the correlator

$K_{dis} = \langle \rho_{s\uparrow} \rho_{s\downarrow} \rangle_{dis} - \langle \rho_{s\uparrow} \rangle_{dis} \langle \rho_{s\downarrow} \rangle_{dis}$ (13) of the operators ρ_s given by Eq. (5). This reflects the duality between interactions and quenched disorder discussed in this paper.

Conclusion. In summary, we have demonstrated equivalence of a class disorder-free systems with attractive interactions to non-interacting disordered systems. The interacting systems that allow for this mapping include dilute quantum gases of trapped ultracold particles and nodal semimetals, where the screening of the interactions is suppressed due to the vanishing DoS near the node.

The mapping constitutes a new approach for describing many-body systems by means of single-particle models. It allows, for example, to simulate numerically many-body effects by diagonalising the Hamiltonians of dual single-particle systems and to predict and classify novel phenomena in each of these classes of systems using the results established for the other class. For example, we have shown that 2D and 3D nodal semimetals with attractive interactions exhibit interaction-driven phase transition in the universality classes of high-dimensional non-Anderson disorder-driven phase transitions that have recently been extensively studied in the context of nodal semimetals and systems with long-range hopping. Furthermore, it has allowed us to find a new non-Anderson disorder-driven transition. Because many-body interacting systems are often described by non-Hermitian Hamiltonians^{25–29}, the equivalence derived here may also be used to classify phase transitions driven by non-Hermitian disorder. We leave, however, a systematic classification of such transitions for future studies.

Acknowledgments. We are grateful to B. Sbierski and L. Radzihovsky for insightful discussions and comments on the manuscript. We have also benefited from discussion with Ya. Rodionov at the early stages of the project.

Appendix A: Mapping for a generic interaction propagator

In this section, we provide the details of the duality between sets diagrams in Figs. 2a and 2d and generalise the duality mapping to the case of an arbitrary spatial and temporal dependencies of the interactions. Basic elements of the diagrammatic technique are shown in Fig. (4). We describe first a generic diagram for an interacting system and demonstrate its equivalents to the corresponding diagram for the non-interacting disordered system. Then we provide explicit expressions for the several lowest-order diagrams in both systems.

The value of each diagram with N interaction propagators is given by

$$(-1)^N \frac{T^{N+1}}{V^{N+1}} \sum_{\omega, \mathbf{p}} \frac{1}{(i\omega_0 - \xi_{\mathbf{p}_0})^2} \frac{1}{i\omega_1 - \xi_{\mathbf{p}_1}} \cdots \frac{1}{i\omega_{2N-1} - \xi_{\mathbf{p}_{2N-1}}} D(\Omega_1, \mathbf{P}_1) \dots D(\Omega_N, \mathbf{P}_N), \quad (\text{A1})$$

where $D(\Omega_i, \mathbf{P}_i)$ is the interaction propagators which depends on the bosonic (fermionic) Matsubara frequency $\Omega_i = 2\pi T n_i$ [$\Omega_i = \pi T(2n_i + 1)$] and momentum \mathbf{P}_i and is the Fourier-transform of the interaction propagator

$$D(\mathbf{r}, \tau; \mathbf{r}', \tau') = - \left\langle T_\tau \hat{\phi}(\mathbf{r}, \tau) \hat{\phi}(\mathbf{r}', \tau') \right\rangle \quad (\text{A2})$$

in the coordinate and Matsubara-time representation, where $\hat{\phi}$ are the bosonic fields corresponding to the interaction between the particles. The summation $\sum_{\omega, \mathbf{p}} \dots$ in Eq. (A1) may be carried out over any N independent frequencies and momenta, with the other frequency and momenta of the particle and interaction propagators determined from the energy and momentum conservation laws in the diagram. We assume the convergence of the sum for each diagram.

In the case of short-ranged unscreened interactions, each interaction propagator is frequency- and momentum-independent and may be replaced by a constant, $D(\Omega_i, \mathbf{P}_i) \rightarrow -g$, given by Eq. (2). In this case, the expression (A1) matches Eq. (6) in the main text. In what follows, we do not assume a specific form of the interaction propagator $D(\Omega, \mathbf{P})$.

Because the bosonic propagator $D(\Omega_i, \mathbf{P}_i)$ is an even function of the Matsubara frequency Ω_i , each summation with respect to Matsubara frequencies ω in Eq. (A1) can be replaced with two summations with respect to ω and $-\omega$, $\sum_{\omega} \dots = \frac{1}{2} \sum_{\omega} \dots + \frac{1}{2} \sum_{-\omega} \dots$, which gives

$$(-1)^N \frac{T^{N+1}}{2V^{N+1}} \sum_{I=0,1} \sum_{\omega, \mathbf{p}} \frac{1}{[(-1)^I i\omega_0 - \xi_{\mathbf{p}_0}]^2} \frac{1}{(-1)^I i\omega_1 - \xi_{\mathbf{p}_1}} \cdots \frac{1}{(-1)^I i\omega_{2N-1} - \xi_{\mathbf{p}_{2N-1}}} D(\Omega_1, \mathbf{P}_1) \dots D(\Omega_N, \mathbf{P}_N). \quad (\text{A3})$$

Below, we compare the expression (A3) for the N -th-order diagram for an interacting disorder-free system to the value of a similar diagram in the equivalent disordered non-interacting system.

In what immediately follows, we assume that the equivalent disordered system described by the Hamiltonian (3) has the volume $V \ell_{d+1}$ in the dimension $d+1$, where ℓ_{d+1} is its length along one dimension and V is the cross section in the remaining d dimensions. The topologically equivalent N -th order diagram is given by

$$\frac{(-1)^N}{\tilde{V}^{N+1} \ell_{d+1}^{N+1}} \sum_{\mathbf{p}, k} \text{Tr} \left[\hat{\sigma}_z \frac{1}{-k_0 \hat{\sigma}_y - \xi_{\mathbf{p}_0} \hat{\sigma}_z} \frac{\hat{\sigma}_z}{2} \frac{1}{-k_0 \hat{\sigma}_y - \xi_{\mathbf{p}_0} \hat{\sigma}_z} \hat{\sigma}_z \cdots \hat{\sigma}_z \frac{1}{-k_{2N-1} \hat{\sigma}_y - \xi_{\mathbf{p}_{2N-1}} \hat{\sigma}_z} \right] \tilde{D}(K_1, \mathbf{P}_1) \dots \tilde{D}(K_N, \mathbf{P}_N), \quad (\text{A4})$$

where (\mathbf{p}_i, k_i) is a $d+1$ -dimensional momentum; $i = 1, 2, \dots, 2N-1$; $\text{Tr} \dots$ is taken with respect to the pseudospin degrees of freedom; $-\tilde{D}(K_i, \mathbf{P}_i)$ is the ‘‘impurity line’’¹¹, the Fourier-transform of the correlator

$$-\tilde{D}(\boldsymbol{\rho} - \boldsymbol{\rho}') = \langle u(\boldsymbol{\rho}) u(\boldsymbol{\rho}') \rangle_{\text{dis}} \quad (\text{A5})$$

of the random potential $u(\boldsymbol{\rho})$. Here, in accordance with the common convention, the impurity line (cf. Fig. 4) is defined to be positive for a real random potential. Similarly to the case of the diagram for the interacting system, the summation in Eq. (A4) may be carried out over any N independent momenta in the dimension $d+1$, while the other momenta of the particle and disorder propagators are determined from the law of momentum conservation. In Eq. A4, we took into account that the the quantity ρ_s , to which the respective diagram contributes, corresponds to the $\hat{\sigma}_z/2$ vertex (see Fig. 4) and to the particle propagator

$$(-k_i \hat{\sigma}_y - \xi_{\mathbf{p}_i} \hat{\sigma}_z)^{-1} = \frac{1}{2} [G^A(k_i, \mathbf{p}_i, E=0) + G^R(k_i, \mathbf{p}_i, E=0)], \quad (\text{A6})$$

where G^A and G^R are the advanced and retarded Green’s functions of a free particle.

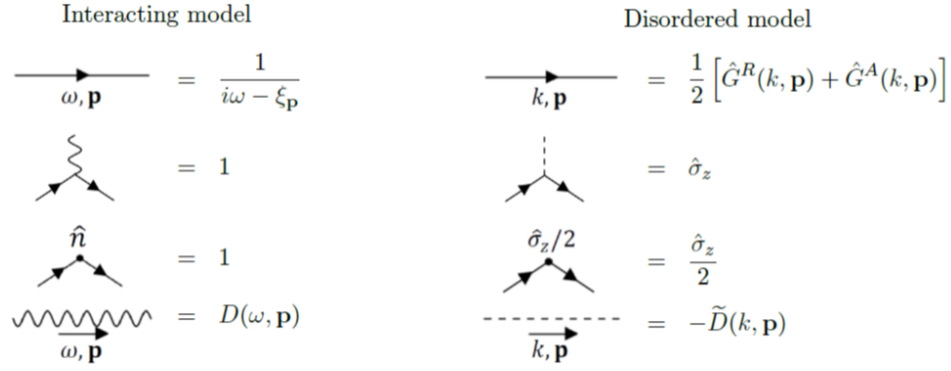


FIG. 4. Elements of the diagrammatic technique for the interacting disorder-free (left) and non-interacting disordered (right) models in momentum space.

Equation (A4) gives

$$\frac{(-1)^N}{2\tilde{V}^{N+1}\ell_{d+1}^{N+1}} \sum_{\mathbf{p}, k} \text{Tr} \left[\frac{1}{ik_0\hat{\sigma}_x - \xi_{\mathbf{p}_0} \mathbb{1}_{2 \times 2}} \frac{1}{ik_0\hat{\sigma}_x - \xi_{\mathbf{p}_0} \mathbb{1}_{2 \times 2}} \cdots \frac{1}{ik_{2N-1}\hat{\sigma}_x - \xi_{\mathbf{p}_{2N-1}} \mathbb{1}_{2 \times 2}} \right] \tilde{D}(K_1, \mathbf{P}_1) \dots \tilde{D}(K_N, \mathbf{P}_N), \quad (\text{A7})$$

where $\mathbb{1}_{2 \times 2}$ is the identity matrix in the pseudospin space. Because the eigenvalues of the operator $\hat{\sigma}_x$ are given by $(-1)^I$ with $I = 0, 1$, Eq. (A7) can be rewritten as

$$\frac{(-1)^N}{2\tilde{V}^{N+1}\ell_{d+1}^{N+1}} \sum_{I=0,1} \sum_{\mathbf{p}, k} \left[\frac{1}{i(-1)^I k_0 - \xi_{\mathbf{p}_0}} \frac{1}{i(-1)^I k_0 - \xi_{\mathbf{p}_0}} \cdots \frac{1}{i(-1)^I k_{2N-1} - \xi_{\mathbf{p}_{2N-1}}} \right] \tilde{D}(K_1, \mathbf{P}_1) \dots \tilde{D}(K_N, \mathbf{P}_N). \quad (\text{A8})$$

Equations (A3) and (A8) for the diagrams for, respectively, the interacting disorder-free and non-interacting disordered systems are identical to each other so long as $\ell_{d+1} = 1/T$ and the Matsubara frequencies ω_i in Eq. (A3) match the values of the momenta k_i in Eq. (A8). The latter condition, with $k_i = 2\pi T n_i$ ($k_i = 2\pi T n_i + \pi T$) and integer n_i , is satisfied if (anti-)periodic boundary conditions are imposed on the disordered system in the case of a (fermionic) bosonic interacting system.

Summary. In summary, we have established the correspondence, to all order of the perturbation theory, between observables in a d -dimensional bosonic (fermionic) interacting disorder-free system at temperature T and a dual $d+1$ -dimensional non-interacting disordered system of length $\ell_{d+1} = 1/T$ with (anti-)periodic boundary conditions along the $d+1$ -st dimension. We focussed on the observable quantities

$$\langle \hat{n}(\mathbf{r}) \rangle = \langle \hat{\rho}_s(\boldsymbol{\rho}) \rangle_{\text{dis}}, \quad (\text{A9})$$

where \hat{n} is the density of particles in the interacting system and the operator ρ_s in the disordered system is defined by Eq. (5). The established equivalence applies, however, to other observables, such as currents and spin/valley degrees of freedom and their correlators. To further illustrate the discussed duality, we consider below the zeroth and first order diagrams contributing to $\langle \hat{n}(\mathbf{r}) \rangle$ and $\langle \hat{\rho}_s(\boldsymbol{\rho}) \rangle_{\text{dis}}$ explicitly.

1. Zeroth order

The concentration of particles at zeroth order is given by

$$\langle \hat{n}^{(0)}(\mathbf{r}) \rangle = \frac{T}{V} \sum'_{\omega, \mathbf{p}} \frac{1}{i\omega - \xi_{\mathbf{p}}} = \frac{1}{V} \sum_{\mathbf{p}} \frac{1}{\exp(\xi_{\mathbf{p}}/T) \mp 1}, \quad (\text{A10})$$

where \sum' is our convention for the regularised sum over Matsubara frequencies (which amounts to, e.g., infinitesimal phase corrections to the frequencies⁷ $i\omega \rightarrow i\omega e^{-i\omega\delta}$), ensuring that the sum of a Matsubara Green's function over frequencies gives the Bose (Fermi) distribution function for bosonic (fermionic) frequencies.

For the disordered system, the zeroth-order contribution to the dual observable is given by

$$\langle \rho_s^{(0)}(\boldsymbol{\rho}) \rangle_{\text{dis}} = \frac{1}{\tilde{V}\ell_{d+1}} \sum'_{\mathbf{p}, k} \text{Tr} \left[\frac{\hat{\sigma}_z}{2} \frac{1}{-k\hat{\sigma}_y - \xi_{\mathbf{p}}\hat{\sigma}_z} \right] = \frac{1}{\tilde{V}\ell_{d+1}} \sum'_{\mathbf{p}, k} \frac{-\xi_{\mathbf{p}}}{k^2 + \xi_{\mathbf{p}}^2} = \frac{1}{\tilde{V}} \sum'_{\mathbf{p}} \frac{1}{\exp(\xi_{\mathbf{p}}\ell_{d+1}) \pm 1}, \quad (\text{A11})$$

where “+” and “-” correspond, respectively, to periodic and antiperiodic boundary conditions along the $d + 1$ -st dimension, resulting in the quantised values $k = 2\pi\ell_{d+1}^{-1}n$ and $k = \pi\ell_{d+1}^{-1}(2n+1)$ of the momentum k . Equations (A10) and (A11) are precisely equivalent for $\ell_{d+1} = 1/T$, in accordance with the duality transformation derived in this paper.

2. First order

Fig. 5a shows the first-order correction to $\langle \hat{n} \rangle$. This diagram contributes

$$-\frac{T^2}{V^2} \sum_{\omega_0, \omega_1, \mathbf{p}_0, \mathbf{p}_1} \frac{1}{(i\omega_0 - \xi_{\mathbf{p}_0})^2} \frac{1}{i\omega_1 - \xi_{\mathbf{p}_1}} D(\omega_0 - \omega_1, \mathbf{p}_0 - \mathbf{p}_1). \quad (\text{A12})$$

Again, because the bosonic propagator is even under the inversion of Matsubara frequency, $D(\omega_0 - \omega_1, \mathbf{p}_0 - \mathbf{p}_1) = D(-\omega_0 + \omega_1, \mathbf{p}_0 - \mathbf{p}_1)$, the sum with respect to the frequencies in Eq.(A12) is equivalent to two sums with respect to ω_0, ω_1 and $-\omega_0, -\omega_1$, $\sum_{\omega_0, \omega_1} \dots = \frac{1}{2} \sum_{\omega_0, \omega_1} \dots + \frac{1}{2} \sum_{-\omega_0, -\omega_1} \dots$. Therefore, Eq.(A12) becomes

$$-\frac{T^2}{2V^2} \sum_{\omega_0, \omega_1, \mathbf{p}_0, \mathbf{p}_1} \left[\frac{1}{(i\omega_0 - \xi_{\mathbf{p}_0})^2} \frac{1}{i\omega_1 - \xi_{\mathbf{p}_1}} + \frac{1}{(-i\omega_0 - \xi_{\mathbf{p}_0})^2} \frac{1}{-i\omega_1 - \xi_{\mathbf{p}_1}} \right] D(\omega_0 - \omega_1, \mathbf{p}_0 - \mathbf{p}_1). \quad (\text{A13})$$

The corresponding diagram for the non-interacting disordered system is shown in Fig. 5b and is given by

$$\begin{aligned} & \frac{1}{\tilde{V}^2 \ell_{d+1}^2} \sum_{\mathbf{p}_0, \mathbf{p}_1, k_0, k_1} \text{Tr} \left[\hat{\sigma}_z \frac{1}{-k_0 \hat{\sigma}_y - \xi_{\mathbf{p}_0} \hat{\sigma}_z} \frac{\hat{\sigma}_z}{2} \frac{1}{-k_0 \hat{\sigma}_y - \xi_{\mathbf{p}_0} \hat{\sigma}_z} \hat{\sigma}_z \frac{1}{-k_1 \hat{\sigma}_y - \xi_{\mathbf{p}_1} \hat{\sigma}_z} \right] \left[-\tilde{D}(k_0 - k_1, \mathbf{p}_0 - \mathbf{p}_1) \right] \\ &= \frac{-1}{2\tilde{V}^2 \ell_{d+1}^2} \sum_{\mathbf{p}_0, \mathbf{p}_1, k_0, k_1} \text{Tr} \left[\frac{1}{ik_0 \hat{\sigma}_x - \xi_{\mathbf{p}_0} \mathbb{1}_{2 \times 2}} \frac{1}{ik_0 \hat{\sigma}_x - \xi_{\mathbf{p}_0} \mathbb{1}_{2 \times 2}} \frac{1}{ik_1 \hat{\sigma}_x - \xi_{\mathbf{p}_0} \mathbb{1}_{2 \times 2}} \right] \tilde{D}(k_0 - k_1, \mathbf{p}_0 - \mathbf{p}_1). \end{aligned} \quad (\text{A14})$$

Taking the trace with respect to the eigenvalues of $\hat{\sigma}_x$ gives

$$\frac{-1}{2\tilde{V}^2 \ell_{d+1}^2} \sum_{\mathbf{p}_0, \mathbf{p}_1, k_0, k_1} \left(\frac{1}{ik_0 - \xi_{\mathbf{p}_0}} \frac{1}{ik_0 - \xi_{\mathbf{p}_0}} \frac{1}{ik_1 - \xi_{\mathbf{p}_0}} + \frac{1}{-ik_0 - \xi_{\mathbf{p}_0}} \frac{1}{-ik_0 - \xi_{\mathbf{p}_0}} \frac{1}{-ik_1 - \xi_{\mathbf{p}_0}} \right) \tilde{D}(k_0 - k_1, \mathbf{p}_0 - \mathbf{p}_1). \quad (\text{A15})$$

Since the values of ω_i and k_i match, due to the choice of the boundary conditions, and $\ell_{d+1} = 1/T$, Eqs. (A13) and (A15) are identical.

Appendix B: Renormalisation-group approach to interacting gases and high-dimensional semimetals

In this section, we describe the renormalisation of interactions in gases of particles with the power-law dispersion $\xi_{\mathbf{k}} \propto k^\alpha$ and the renormalisation of disorder in the dual class of systems, i.e. semimetals with the dispersion $\xi_{\mathbf{k}} \hat{\sigma}_z + k_{d+1} \hat{\sigma}_y$. We demonstrate that these renormalisation are described by the same RG flow equation (9), which illustrates that these systems exhibit interaction-driven (disorder-driven) phase transitions in the same universality class.

The RG procedure for the interacting system involves repeatedly integrating out shells of largest momenta and frequencies,

$$K e^{-l} \ll |\mathbf{k}| \ll K, \quad (\text{B1a})$$

$$|\xi_{K e^{-l}}| \ll \omega \ll |\xi_K|, \quad (\text{B1b})$$

and renormalising the properties of the systems perturbatively in the coupling constant g . The details of the cutoff procedure are not important in the one-loop approximation for the dimension d near the critical dimension $d_c = \alpha$. The diagrams for the one-loop renormalisation of the interaction propagator are shown in Fig. 6a-e. When evaluating them, it is sufficient to set all external incoming and outgoing frequencies and momenta to zero and sum/integrate only with respect to intermediate frequencies and momenta. The main contribution comes from diagram 6c:

$$[6c] = g^2 T \sum_{i\omega} \int_{\mathbf{k}} \frac{1}{i\omega - \hat{\xi}_{\mathbf{k}}} \otimes \frac{1}{-i\omega - \hat{\xi}_{-\mathbf{k}}}, \quad (\text{B2})$$

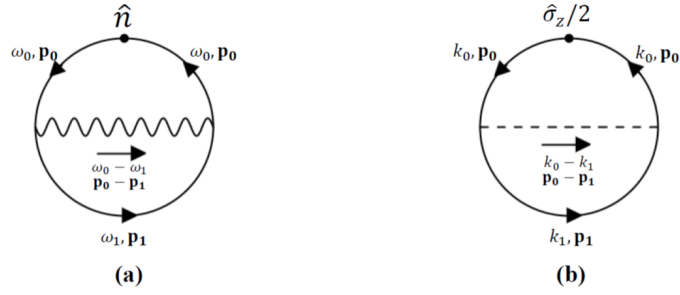


FIG. 5. First-order diagrams for the density \hat{n} in interacting disorder-free (a) and the operator ρ_s in non-interacting disordered (b) systems.

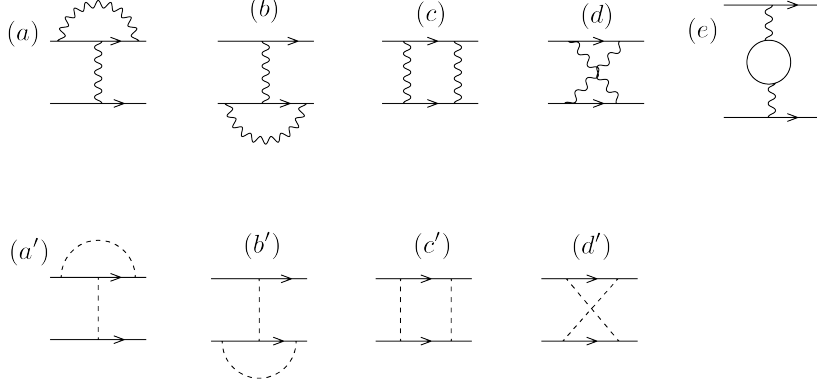


FIG. 6. Diagrams for the renormalisation of the coupling constants in an interacting disorder-free (a – e) and non-interacting disordered (a' – d') systems.

where the frequency summation and integration with respect to the momentum \mathbf{k} are carried out over the intervals (B1a)-(B1b); $\int_{\mathbf{k}} \dots = \int \frac{d^d \mathbf{k}}{(2\pi)^d} \dots$; the dispersion $\xi_{\mathbf{k}} \propto k^\alpha$ has the power dependence on the momentum \mathbf{k} , but may also have additional structure in the valley or spin space; \otimes is the product of the spin/valley subspaces corresponding to the top and bottom propagators in Fig. (6)c.

We consider the case of large ultraviolet momentum cutoffs K and Ke^{-l} , corresponding to the kinetic energies significantly exceeding the temperature T . This allows us to replace the summation with respect to frequencies in Eq. (B2) by integration, $T \sum_{i\omega} \dots \rightarrow \int \frac{d\omega}{2\pi} \dots$. For a scalar dispersion

$$\xi_{\mathbf{k}} = |\mathbf{k}|^\alpha, \quad (\text{B3})$$

which has no valley and spin structure, the renormalised interaction propagator also has a trivial structure ($\propto \mathbf{1} \otimes \mathbf{1}$) in the spin/valley space, and the value of diagram 6c is given by

$$[6c] = \frac{g^2 S_d K^{d-\alpha}}{2(2\pi)^d} \frac{1 - e^{-(d-\alpha)l}}{d - \alpha}. \quad (\text{B4})$$

All the other contributions shown in Fig. 6 may be estimated as

$$[6a] \sim [6b] \sim [6d] \sim [6e] \sim \frac{g^2 S_d K^{d-\alpha}}{2(2\pi)^d} \quad (\text{B5})$$

and are suppressed for the dimensions d close to the critical dimension $d_c = \alpha$. This leads to the RG flow equation for the coupling g given by

$$\partial_l g = \frac{S_d K^{d-\alpha}}{2(2\pi)^d} g^2. \quad (\text{B6})$$

Introducing the dimensionless coupling constant

$$\gamma = \frac{S_d}{2(2\pi)^d} g K^{d-\alpha} \quad (\text{B7})$$

gives the one-loop RG flow equation

$$\partial_t \gamma = (\alpha - d)\gamma + \gamma^2. \quad (\text{B8})$$

It is possible to show that the RG flow equation (B8) is exact, i.e. applies beyond the one-loop approximation. It has been noticed in Ref. 56 that the renormalised contact interaction between quadratically dispersive bosonic particles is given by the ladder diagrams shown in Fig. (7) and is, therefore, corresponding to the solution of the RG equation (B8). This result can be straightforwardly generalised to the case of the power-law dispersion $\xi_{\mathbf{k}} = k^\alpha$ considered here. The RG flow is terminated at the value of the ultraviolet cutoff K equal to the inverse size L^{-1} or a characteristic momentum scale corresponding to the renormalised kinetic energy on the order of the temperature T or the chemical potential μ .

The diagrams for the renormalisation in the dual disordered non-interacting system, described by the Hamiltonian (3), are shown in Figure 6a' - d'. They are topologically equivalent to diagrams 6a - d and do not include a diagram with a closed loop of particle propagators. In the diagrammatic technique for the disordered systems¹¹, contributions with loops are absent by construction. Although such loops are present for the interacting systems we consider, their contribution is suppressed due to the suppressed density of states at the chemical potential assumed in this paper.

The main contribution to the renormalisation of the coupling g in the disordered system comes from diagram 6c'. While the other contributions to the renormalisation are suppressed, it is convenient to evaluate together diagrams 6c' and 6d':

$$\begin{aligned} 6c' + 6d' &= g^2 \int_{\mathbf{p}} \int_{p_{d+1}} \hat{\sigma}_z \left(\frac{1}{\xi_{\mathbf{p}} \hat{\sigma}_z + p_{d+1} \hat{\sigma}_y} + \frac{1}{\xi_{-\mathbf{p}} \hat{\sigma}_z - p_{d+1} \hat{\sigma}_y} \right) \hat{\sigma}_z \otimes \hat{\sigma}_z \frac{1}{\xi_{\mathbf{p}} \hat{\sigma}_z + p_{d+1} \hat{\sigma}_y} \hat{\sigma}_z \\ &= g^2 \int_{\mathbf{p}} \int_{p_{d+1}} \frac{2\xi_{\mathbf{p}} \hat{\sigma}_z}{\xi_{\mathbf{p}}^2 + p_{d+1}^2} \otimes \frac{\hat{\sigma}_z (\xi_{\mathbf{p}} \hat{\sigma}_z + p_{d+1} \hat{\sigma}_y) \hat{\sigma}_z}{\xi_{\mathbf{p}}^2 + p_{d+1}^2} = g^2 \int_{\mathbf{p}} \int_{p_{d+1}} \frac{2\xi_{\mathbf{p}}^2}{[\xi_{\mathbf{p}}^2 + p_{d+1}^2]^2} \hat{\sigma}_z \otimes \hat{\sigma}_z \\ &\approx \frac{g^2 S_d K^{d-\alpha}}{2(2\pi)^d} \frac{1 - e^{-(d-\alpha)t}}{d - \alpha}. \end{aligned} \quad (\text{B9})$$

Similarly to the case of interacting systems, it is possible to demonstrate that the contributions of the other diagrams to the renormalisation of the coupling g are suppressed, and the flow of the coupling is again described by Eq. (B8). Identical RG flows for the coupling in the cases of interacting disorder-free and non-interacting disordered systems illustrate the equivalence between the two classes of systems discussed in this paper.

Both of these classes of systems display transitions at the critical value of the dimensionless coupling $\gamma_c = (\alpha - d)^{-1}$ between the phases with irrelevant interactions (disorder), for subcritical coupling, and relevant interactions (disorder), for supercritical interactions (disorder). We emphasise that the phenomenology of such transitions is similar to the phenomenology of the non-Anderson disorder-driven transitions¹⁴ studied previously for systems with isotropic dispersions $\xi_{\mathbf{k}} \propto k^{\tilde{d}}$ in dimensions $\tilde{d} > 2\delta$: renormalised disorder in such systems vanishes for subcritical values of the disorder strength and is finite otherwise. The RG equations for the flow of the dimensionless disorder strength for such systems are given by

$$\partial_t \gamma = (2\delta - \tilde{d})\gamma + \gamma^2 + \mathcal{O}(\gamma^3) \quad (\text{B10})$$

and in one loop are also given by the diagrams shown in Fig. 6a' - d'. We emphasise that for generic symmetries of quenched disorder all of these four diagrams may give contributions of the same order of magnitude to the renormalisation and the higher-loop contributions and in general are non-negligible (see, e.g., Ref. 43).

The disorder-driven transitions considered in this paper, equivalent to the interaction-driven transitions in interacting systems, are an extension of the previously studied non-Anderson disorder-driven transitions to the case of systems with an anisotropic dispersion $\propto \hat{\sigma}_z \xi_{\mathbf{p}} + \hat{\sigma}_y p_{d+1}$, which is linear along one direction and has a power-law form $\xi_{\mathbf{p}} \propto p^\alpha$ along the other d dimensions. The lower-critical dimension for the non-Anderson disorder-driven transitions in such systems is given by $\tilde{d} \equiv d + 1 = \alpha + 1$. The vanishing of the high-order contributions in the RG flow (B8) is a consequence of the disorder symmetry ($\propto u \hat{\sigma}_z$) in such systems.

Appendix C: Details of the duality between quantum dot and 1D wires

In this section, we provide the details of the duality mapping between the one-site Hubbard model (quantum dot) described by the Hamiltonian (10) and a disordered 1D wire described by the Hamiltonian (11). The Hamiltonian of

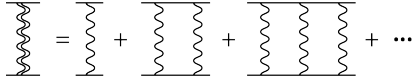


FIG. 7. Ladder diagrams for the renormalisation of the interaction between bosonic particles in vacuum.

the quantum dot can be rewritten in the equivalent form

$$\hat{\mathcal{H}}_{dot} = \xi \hat{n}_\uparrow + \xi \hat{n}_\downarrow - g \hat{n}_\uparrow \hat{n}_\downarrow = \left(\xi + \frac{g}{2} \right) \hat{n}_\uparrow + \left(\xi + \frac{g}{2} \right) \hat{n}_\downarrow - \frac{g}{2} (\hat{n}_\uparrow + \hat{n}_\downarrow)^2, \quad (\text{C1})$$

where we have used that $\hat{n}_{\uparrow,\downarrow}^2 \equiv \hat{n}_{\uparrow,\downarrow}$. Observables in a system described by the Hamiltonian (C1) can be represented in the form of a path integral over Grassmann variables

$$\langle \dots \rangle = \int \mathcal{D}\bar{\Psi} \mathcal{D}\Psi \dots \exp \left\{ - \int_0^\beta \sum_{i=\uparrow,\downarrow} \bar{\Psi}_i(\tau) \left[\partial_\tau + \xi + \frac{g}{2} \right] \Psi_i(\tau) d\tau - \frac{1}{2g} \int_0^\beta \left[\sum_{i=\uparrow,\downarrow} \bar{\Psi}_i(\tau) \Psi_i(\tau) \right]^2 d\tau \right\}, \quad (\text{C2})$$

where the preexponential \dots corresponds to the operator of the observable expressed in terms of the Grassmann fields $\bar{\Psi}$ and Ψ . Decoupling the quartic term by a bosonic field ϕ gives

$$\langle \dots \rangle = \int \mathcal{D}\bar{\Psi} \mathcal{D}\Psi \dots \exp \left\{ - \int_0^\beta \sum_{i=\uparrow,\downarrow} \bar{\Psi}_i(\tau) \left[\partial_\tau + \xi + \frac{g}{2} \right] \Psi_i(\tau) d\tau - \frac{1}{2g} \int_0^\beta \phi^2(\tau) d\tau \right\}. \quad (\text{C3})$$

The action describing the observable in Eq. (C3) corresponds to spin-1/2 fermions interacting with bosons whose propagator is given by $\langle \phi(\tau) \phi(\tau') \rangle = g \delta(\tau - \tau')$.

Applying the duality transformation developed in this paper, this model may be mapped to a 1D model with quenched disorder, with the Matsubara time τ mapped to the coordinate x of the 1D model and with the bosonic field $\phi(\tau)$ mapped to a random potential $u(x)$. The Hamiltonian of this 1D model is given by

$$\hat{\mathcal{H}}_{wire} = \sum_{i=\uparrow,\downarrow} \hat{\Psi}_i(x) [\xi \hat{\sigma}_z - i \hat{\sigma}_y \partial_x + u(x) \hat{\sigma}_z] \hat{\Psi}_i(x). \quad (\text{C4})$$

We emphasise that, strictly speaking, the quantum dot described by the Hamiltonian (C1) does not satisfy the assumptions about the negligibility of screening and Hartree-type contributions, which correspond to diagrams with additional fermionic loops and are neglected in this paper when deriving the equivalence between interacting disorder-free and non-interacting disordered systems. For example, diagram (a) in Fig. 8 describes the Hartree contribution to the average occupation number $\langle \hat{n}_\sigma \rangle$ for the electron state with spin σ and is equal to diagram (b), which we take into account when demonstrating the equivalence, and is, therefore, non-negligible.

However, observables in the quantum dot may still be mapped to observables in the disordered wire so long as they are unaffected by the screening and Hartree contributions. To illustrate this, we consider the leading contribution to the correlator

$$K = \langle \hat{n}_\uparrow \hat{n}_\downarrow \rangle - \langle \hat{n}_\uparrow \rangle \langle \hat{n}_\downarrow \rangle \quad (\text{C5})$$

of the occupation numbers with different spins in the quantum dot. In the equilibrium state at temperature T , the correlator is given by

$$K = \frac{\sum_{n_{\uparrow,\downarrow}=0,1} n_\uparrow n_\downarrow e^{-\frac{n_\uparrow \xi + n_\downarrow \xi - g n_\uparrow n_\downarrow}{T}}}{\sum_{n_{\uparrow,\downarrow}=0,1} e^{-\frac{n_\uparrow \xi + n_\downarrow \xi - g n_\uparrow n_\downarrow}{T}}} - \left(\frac{\sum_{n_{\uparrow,\downarrow}=0,1} n_\uparrow e^{-\frac{n_\uparrow \xi + n_\downarrow \xi - g n_\uparrow n_\downarrow}{T}}}{\sum_{n_{\uparrow,\downarrow}=0,1} e^{-\frac{n_\uparrow \xi + n_\downarrow \xi - g n_\uparrow n_\downarrow}{T}}} \right)^2 \quad (\text{C6})$$

$$\approx \frac{g}{T} \left[\frac{e^{\xi/T}}{(1 + e^{\xi/T})^2} \right]^2, \quad (\text{C7})$$

where we kept only the leading in g contribution. The correlator (C5) can also be found diagrammatically, as shown in Fig. 8. The leading in the coupling g contribution is given by diagram (c):

$$K \approx \text{Diagram (c)} = gT^3 \sum_{\omega_1, \omega_2} \frac{1}{(i\omega_1 - \xi)^2} \frac{1}{(i\omega_2 - \xi)^2} = \frac{g}{T} \left[\frac{e^{\xi/T}}{(1 + e^{\xi/T})^2} \right]^2. \quad (\text{C8})$$

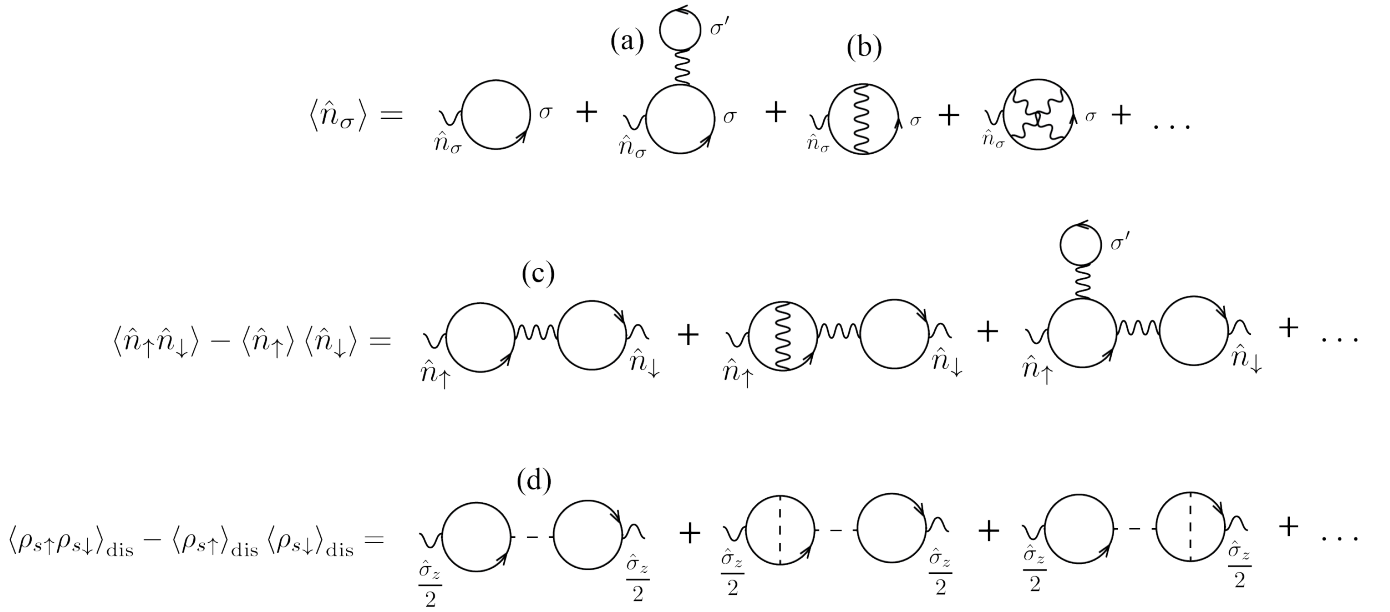


FIG. 8. Diagrams that contribute to the correlators K and K_{dis} in the one-site Hubbard model and a disordered wire described by the Hamiltonians (C1) and (C4).

Because this contribution does not contain fermionic loops mimicking the screening of the interactions or Hartree contributions, it allows for a mapping to a similar correlator

$$K_{\text{dis}} = \langle \rho_{s\uparrow} \rho_{s\downarrow} \rangle_{\text{dis}} - \langle \rho_{s\uparrow} \rangle_{\text{dis}} \langle \rho_{s\downarrow} \rangle_{\text{dis}}. \quad (\text{C9})$$

in a disordered wire described by the Hamiltonian (C4). The diagrams for the correlator in the disordered system are shown in Fig. 8, where the leading-order contribution is given by diagram (d):

$$\begin{aligned}
K_{\text{dis}} &\approx \text{Diagram (d)} \\
&= \frac{g}{\ell_{d+1}^3} \sum_{k_1, k_2} \text{Tr} \left[\hat{\sigma}_z \frac{1}{-k_1 \hat{\sigma}_y - \xi \hat{\sigma}_z} \frac{\hat{\sigma}_z}{2} \frac{1}{-k_1 \hat{\sigma}_y - \xi \hat{\sigma}_z} \right] \text{Tr} \left[\hat{\sigma}_z \frac{1}{-k_2 \hat{\sigma}_y - \xi \hat{\sigma}_z} \frac{\hat{\sigma}_z}{2} \frac{1}{-k_2 \hat{\sigma}_y - \xi \hat{\sigma}_z} \right] \\
&= \frac{g}{\ell_{d+1}^3} \sum_{k_1, k_2} \frac{-k_1^2 + \xi^2}{(k_1^2 + \xi^2)^2} \frac{-k_2^2 + \xi^2}{(k_2^2 + \xi^2)^2} = g \ell_{d+1} \left[\frac{e^{\xi \ell_{d+1}}}{(1 + e^{\xi \ell_{d+1}})^2} \right]^2. \quad (\text{C10})
\end{aligned}$$

Because the quantum dot described by the Hamiltonian (C1) is fermionic, the dual to it disordered wire described by the Hamiltonian (C4) has antiperiodic boundary conditions. At $\ell_{d+1} = 1/T$, Eqs. (C8) and (C10) for observables in, respectively, the quantum dot and the disordered wire are equivalent, which illustrates again the interactions-disorder duality shown in this paper.

¹ R. Blankenbecler, D. J. Scalapino, and R. L. Sugar, “Monte Carlo calculations of coupled boson-fermion systems. I,” *Phys. Rev. D* **24**, 2278–2286 (1981).

² J. E. Hirsch, “Discrete Hubbard-Stratonovich transformation for fermion lattice models,” *Phys. Rev. B* **28**, 4059–4061 (1983).

³ S. R. White, D. J. Scalapino, R. L. Sugar, N. E. Bickers, and R. T. Scalettar, “Attractive and repulsive pairing interaction vertices for the two-dimensional Hubbard model,” *Phys. Rev. B* **39**, 839–842 (1989).

⁴ K. B. Efetov, *Supersymmetry in Disorder and Chaos* (Cambridge University Press, New York, 1999).

- ⁵ A. Kamenev, *Field Theory of Non-Equilibrium Systems* (Cambridge Univ. Press, Cambridge, 2011).
- ⁶ D. Belitz and T. R. Kirkpatrick, “The Anderson-Mott transition,” *Rev. Mod. Phys.* **66**, 261–380 (1994).
- ⁷ A. Altland and B. Simons, *Condensed Matter Field Theory* (Leiden: Cambridge University Press, 2006).
- ⁸ M. Schütt, P. M. Ostrovsky, I. V. Gornyi, and A. D. Mirlin, “Coulomb interaction in graphene: Relaxation rates and transport,” *Phys. Rev. B* **83**, 155441 (2011).
- ⁹ Pavan Hosur, S. A. Parameswaran, and Ashvin Vishwanath, “Charge Transport in Weyl Semimetals,” *Phys. Rev. Lett.* **108**, 046602 (2012).
- ¹⁰ While calculations⁹ neglecting the screening give the correct result for the temperature dependence of the conductivity $\sigma \sim \frac{e^2 T}{v_F \alpha^2}$, where $\alpha = \frac{e^2}{v_F \epsilon}$ is the “fine-structure constant”, as follows from dimensional considerations, it still remains to be established, to our knowledge, if such an approximation gives the correct numerical coefficient.
- ¹¹ A. A. Abrikosov, L. P. Gorkov, and I. E. Dzyaloshinski, *Methods of Quantum Field Theory in Statistical Physics* (Dover, New York, 1975).
- ¹² Eduardo Fradkin, “Critical behavior of disordered degenerate semiconductors. I. Models, symmetries, and formalism,” *Phys. Rev. B* **33**, 3257–3262 (1986).
- ¹³ Eduardo Fradkin, “Critical behavior of disordered degenerate semiconductors. II. Spectrum and transport properties in mean-field theory,” *Phys. Rev. B* **33**, 3263–3268 (1986).
- ¹⁴ S. V. Syzranov and L. Radzihovsky, “High-Dimensional Disorder-Driven Phenomena in Weyl Semimetals, Semiconductors, and Related Systems,” *Annu. Rev. Cond. Mat. Phys.* **9**, 33–58 (2018).
- ¹⁵ A. Rodríguez, V. A. Malyshev, G. Sierra, M. A. Martín-Delgado, J. Rodríguez-Laguna, and F. Domínguez-Adame, “Anderson Transition in Low-Dimensional Disordered Systems Driven by Long-Range Nonrandom Hopping,” *Phys. Rev. Lett.* **90**, 027404 (2003).
- ¹⁶ A. V. Malyshev, V. A. Malyshev, and F. Domínguez-Adame, “Monitoring the localization-delocalization transition within a one-dimensional model with nonrandom long-range interaction,” *Phys. Rev. B* **70**, 172202 (2004).
- ¹⁷ S. V. Syzranov, L. Radzihovsky, and V. Gurarie, “Critical Transport in Weakly Disordered Semiconductors and Semimetals,” *Phys. Rev. Lett.* **114**, 166601 (2015).
- ¹⁸ S. V. Syzranov, V. Gurarie, and L. Radzihovsky, “Unconventional localisation transition in high dimensions,” *Phys. Rev. B* **91**, 035133 (2015).
- ¹⁹ Philip Richerme, Zhe-Xuan Gong, Aaron Lee, Crystal Senko, Jacob Smith, Michael Foss-Feig, Spyridon Michalakis, Alexey V. Gorshkov, and Christopher Monroe, “Non-local propagation of correlations in quantum systems with long-range interactions,” *Nature Lett.* **511**, 198–201 (2014).
- ²⁰ R. Islam, C. Senko, W. C. Campbell, S. Korenblit, J. Smith, A. Lee, E. E. Edwards, C.-C. J. Wang, J. K. Freericks, and C. Monroe, “Emergence and Frustration of Magnetism with Variable-Range Interactions in a Quantum Simulator,” *Science* **340**, 583–587 (2013).
- ²¹ P. Jurcevic, B. P. Lanyon, P. Hauke, C. Hempel, P. Zoller, R. Blatt, and C. F. Roos, “Quasiparticle engineering and entanglement propagation in a quantum many-body system,” *Nature* **511**, 202–205 (2014).
- ²² P. Jurcevic, P. Hauke, C. Maier, C. Hempel, B. P. Lanyon, R. Blatt, and C. F. Roos, “Spectroscopy of Interacting Quasiparticles in Trapped Ions,” *Phys. Rev. Lett.* **115**, 100501 (2015).
- ²³ Konstantin S. Tikhonov and Mikhail V. Feigel’man, “Strange metal state near quantum superconductor-metal transition in thin films,” *Annals of Physics* **417**, 168138 (2020), eliashberg theory at 60: Strong-coupling superconductivity and beyond.
- ²⁴ S. V. Syzranov and V. Gurarie, “Duality between disordered nodal semimetals and systems with power-law hopping,” *Phys. Rev. Research* **1**, 032035 (2019).
- ²⁵ Vladimir V. Konotop, Jianke Yang, and Dmitry A. Zezyulin, “Nonlinear waves in \mathcal{PT} -symmetric systems,” *Rev. Mod. Phys.* **88**, 035002 (2016).
- ²⁶ Tsuneya Yoshida, Robert Peters, Norio Kawakami, and Yasuhiro Hatsugai, “Exceptional band touching for strongly correlated systems in equilibrium,” arXiv e-prints, arXiv:2002.11265 (2020), arXiv:2002.11265 [cond-mat.str-el].
- ²⁷ H Varguet, B Rousseaux, D Dzsozjan, H R Jauslin, S Guérin, and G Colas des Francs, “Non-hermitian Hamiltonian description for quantum plasmonics: from dissipative dressed atom picture to Fano states,” *Journal of Physics B: Atomic, Molecular and Optical Physics* **52**, 055404 (2019).
- ²⁸ Huitao Shen, Bo Zhen, and Liang Fu, “Topological Band Theory for Non-Hermitian Hamiltonians,” *Phys. Rev. Lett.* **120**, 146402 (2018).
- ²⁹ Naomichi Hatano and David R. Nelson, “Vortex pinning and non-Hermitian quantum mechanics,” *Phys. Rev. B* **56**, 8651–8673 (1997).
- ³⁰ Tobias Meng and Leon Balents, “Weyl superconductors,” *Phys. Rev. B* **86**, 054504 (2012).
- ³¹ Joseph Maciejko and Rahul Nandkishore, “Weyl semimetals with short-range interactions,” *Phys. Rev. B* **90**, 035126 (2014).
- ³² Huazhou Wei, Sung-Po Chao, and Vivek Aji, “Excitonic Phases from Weyl Semimetals,” *Phys. Rev. Lett.* **109**, 196403 (2012).
- ³³ Huazhou Wei, Sung-Po Chao, and Vivek Aji, “Odd-parity superconductivity in Weyl semimetals,” *Phys. Rev. B* **89**, 014506 (2014).
- ³⁴ Gil Young Cho, Jens H. Bardarson, Yuan-Ming Lu, and Joel E. Moore, “Superconductivity of doped Weyl semimetals: Finite-momentum pairing and electronic analog of the $^3\text{He-A}$ phase,” *Phys. Rev. B* **86**, 214514 (2012).
- ³⁵ Maximilian Trescher, Emil J. Bergholtz, Masafumi Udagawa, and Johannes Knolle, “Charge density wave instabilities of type-II Weyl semimetals in a strong magnetic field,” *Phys. Rev. B* **96**, 201101 (2017).
- ³⁶ Wujun Shi, Benjamin J. Wieder, Holger L. Meyerheim, Yan Sun, Yang Zhang, Yiwei Li, Lei Shen, Yanpeng Qi, Lexian Yang, Jagannath Jena, Peter Werner, Klaus Koepf, Stuart Parkin, Yulin Chen, Claudia Felser, B. Andrei Bernevig, and Zhijun Wang, “A charge-density-wave topological semimetal,” *Nature Physics* **17**, 381–387 (2021).
- ³⁷ Ryuichi Shindou and Shuichi Murakami, “Effects of disorder in three-dimensional Z_2 quantum spin Hall systems,” *Phys. Rev. B* **79**, 045321 (2009).
- ³⁸ Pallab Goswami and Sudip Chakravarty, “Quantum Criticality between Topological and Band Insulators in 3 + 1 Dimensions,” *Phys. Rev. Lett.* **107**, 196803 (2011).
- ³⁹ Shinsei Ryu and Kentaro Nomura, “Disorder-induced quantum phase transitions in three-dimensional topolog-

- ical insulators and superconductors,” *Phys. Rev. B* **85**, 155138 (2012).
- ⁴⁰ Koji Kobayashi, Tomi Ohtsuki, Ken-Ichiro Imura, and Igor F. Herbut, “Density of States Scaling at the Semimetal to Metal Transition in Three Dimensional Topological Insulators,” *Phys. Rev. Lett.* **112**, 016402 (2014).
- ⁴¹ T. Louvet, D. Carpentier, and A. A. Fedorenko, “On the disorder-driven quantum transition in three-dimensional relativistic metals,” *Phys. Rev. B* **94**, 220201 (2016).
- ⁴² Bitan Roy, Robert-Jan Slager, and Vladimir Juričić, “Global Phase Diagram of a Dirty Weyl Liquid and Emergent Superuniversality,” *Phys. Rev. X* **8**, 031076 (2018).
- ⁴³ S. V. Syzranov, P. M. Ostrovsky, V. Gurarie, and L. Radzihovsky, “Critical exponents at the unconventional disorder-driven transition in a Weyl semimetal,” *Phys. Rev. B* **93**, 155113 (2016).
- ⁴⁴ J. H. Pixley, D. A. Huse, and S. Das Sarma, “Rare-Region-Induced Avoided Quantum Criticality in Disordered Three-Dimensional Dirac and Weyl Semimetals,” *Physical Review X* **6**, 021042 (2016).
- ⁴⁵ Björn Sbierski, Emil J. Bergholtz, and Piet W. Brouwer, “Quantum critical exponents for a disordered three-dimensional Weyl node,” *Phys. Rev. B* **92**, 115145 (2015).
- ⁴⁶ Soumya Bera, Jay D. Sau, and Bitan Roy, “Dirty Weyl semimetals: Stability, phase transition, and quantum criticality,” *Phys. Rev. B* **93**, 201302 (2016).
- ⁴⁷ B. Sbierski, K. S. C. Decker, and P. W. Brouwer, “Weyl node with random vector potential,” *Phys. Rev. B* **94**, 220202 (2016).
- ⁴⁸ Shang Liu, Tomi Ohtsuki, and Ryuichi Shindou, “Effect of disorder in three dimensional layered Chern insulator,” *Phys. Rev. Lett.* **116**, 066401 (2016).
- ⁴⁹ Ivan Balog, David Carpentier, and Andrei A. Fedorenko, “Disorder-Driven Quantum Transition in Relativistic Semimetals: Functional Renormalization via the Porous Medium Equation,” *Phys. Rev. Lett.* **121**, 166402 (2018), 1710.07932.
- ⁵⁰ Xunlong Luo, Baolong Xu, Tomi Ohtsuki, and Ryuichi Shindou, “Quantum multicriticality in disordered Weyl semimetals,” *Phys. Rev. B* **97**, 045129 (2018).
- ⁵¹ F. Wegner, “Bounds on the density of states in disordered systems,” *Z. Phys. B* **44**, 9–15 (1981).
- ⁵² I. M. Suslov, “Density of states near an Anderson transition in four-dimensional space: Lattice mode,” *Sov. Phys. JETP* **79**, 307–320 (1994).
- ⁵³ Rahul Nandkishore, David A. Huse, and S. L. Sondhi, “Rare region effects dominate weakly disordered 3D Dirac points,” *Phys. Rev. B* **89**, 245110 (2014).
- ⁵⁴ Justin H. Wilson, David A. Huse, S. Das Sarma, and J. H. Pixley, “Avoided quantum criticality in exact numerical simulations of a single disordered Weyl cone,” *Phys. Rev. B* **102**, 100201 (2020).
- ⁵⁵ J. H. Pixley and Justin H. Wilson, “Rare regions and avoided quantum criticality in disordered Weyl semimetals and superconductors,” (2021), arXiv:2102.02822 [cond-mat.dis-nn].
- ⁵⁶ D.I. Uzunov, “On the zero temperature critical behaviour of the nonideal Bose gas,” *Physics Letters A* **87**, 11–14 (1981).
- ⁵⁷ V. Gurarie and L. Radzihovsky, “Resonantly paired fermionic superfluids,” *Annals of Physics* **322**, 2–119 (2007), january Special Issue 2007.
- ⁵⁸ Predrag Nikolic and Subir Sachdev, “Renormalization-group fixed points, universal phase diagram, and $1/N$ expansion for quantum liquids with interactions near the unitarity limit,” *Phys. Rev. A* **75**, 033608 (2007).
- ⁵⁹ Martin Y. Veillette, Daniel E. Sheehy, and Leo Radzihovsky, “Large- N expansion for unitary superfluid Fermi gases,” *Phys. Rev. A* **75**, 043614 (2007).
- ⁶⁰ Björn Sbierski and Sergey Syzranov, “Non-Anderson critical scaling of the Thouless conductance in 1D,” *Annals of Physics* **418**, 168169 (2020).